P6M.3

Influence of elevated heating on the Zagros Plateau (Iran) on circulations in Southwest Asia

Benjamin F Zaitchik*
Ronald B Smith
Yale University, New Haven, CT

Introduction

The summertime atmospheric circulation in Southwest Asia is characterized by persistent subsidence in the free troposphere. This subsidence is primarily a product of global circulations involving the Hadley Cell and the Asian Monsoon (Rodwell and Hoskins, 1996), but the distribution and intensity of descent within the region is influenced by local geography. The Zagros Plateau of Iran, in particular, is a large elevated heat source that may affect patterns of subsidence and associated atmospheric stability. In GCM and Global Reanalyses datasets the Zagros plateau stands out as a region of unusually high temperature up to and above 500mb. This temperature feature is greatest in the summertime, when both plateau heating and regional subsidence are at a maximum.

A regional climate model was used to simulate the influence of plateau heating on summertime circulations in Southwest Asia for 1999 and 2003, a particularly dry year and a moderately wet year, respectively. In the CONTROL simulation the model was driven using standard global datasets. In a MTSNOW simulation all datasets were standard except that the albedo on the Zagros Plateau was fixed at a snow-like 0.9 in order to neutralize surface heating (Figure 1). Comparisons between the CONTROL and MTSNOW simulations indicate that heating on the Zagros plateau is responsible for a persistent temperature anomaly throughout the troposphere in the summer months (Figure 2). This anomaly is associated with a steady heat-driven circulation tendency that causes southerly (warming) advection over the Zagros and northerly (cooling) advection over the Levant and the Mediterranean coast. Cool advection in the Levant is associated with adiabatic descent on the order of 0.2 – 0.3 Pa s^{-1} in the summer months. In the MTSNOW simulation several well-known features of summertime climatology in the region—the "Persian Trough" low pressure system, a persistent low-level inversion in the Levant, and the near-surface northwesterly *Etesian* winds—were reduced or eliminated. Model comparisons also indicate that Plateau heating inhibits cloud formation within the basin and has an influence on summertime vapor flux and precipitation events.

These MM5 results provide some insight as to the influence that the Zagros Plateau has on regional climate. The very realism of these simulations, however, can make it difficult to understand the physics responsible for model results. Here we present two simplified models of Zagros heating for which closed form solutions can be obtained. The first model considers topographic and heat-induced forcing in the presence of a vertical wind shear, while the second neglects topography and shear but allows internal heating to vary as a continuous function of altitude. The sheared model successfully replicates the persistent downstream anti-cyclone produced in MM5 simulations but fails to return a realistic surface low in the vicinity of heating. The model without shear captures the vertical structure associated with heating—low pressure at the surface and high pressure aloft—but cannot adequately replicate the downstream advection of the atmospheric response. Neither model captures the persistent *upstream* low pressure center that is produced in MM5 simulations. This upstream heat response may not be amenable to a linear explanation.

*Corresponding Author Address: Benjamin Zaitchik, Department of Geology & Geophysics, Yale University PO Box 208109, New Haven, CT 06520; email: benjamin.zaitchik@yale.edu

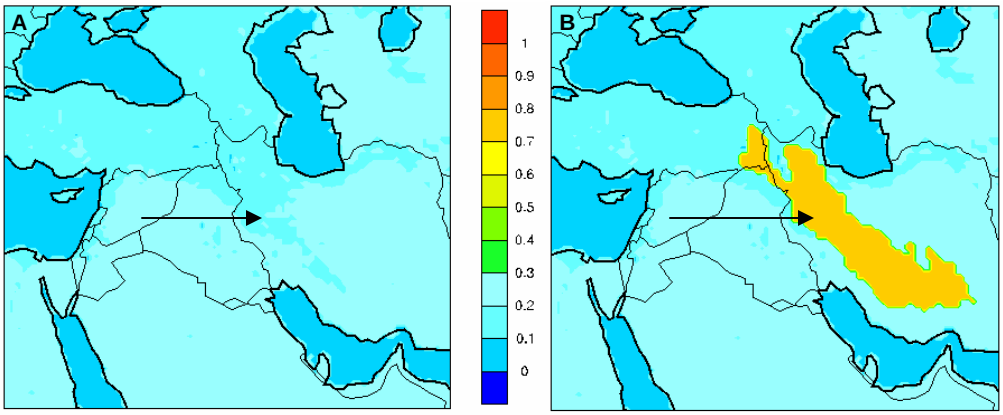

Figure 1: Average July-August albedo for (A) CONTROL and (B) MTSNOW MM5 simulations (unitless). Arrows indicate the mean background wind, which is approximately westerly.

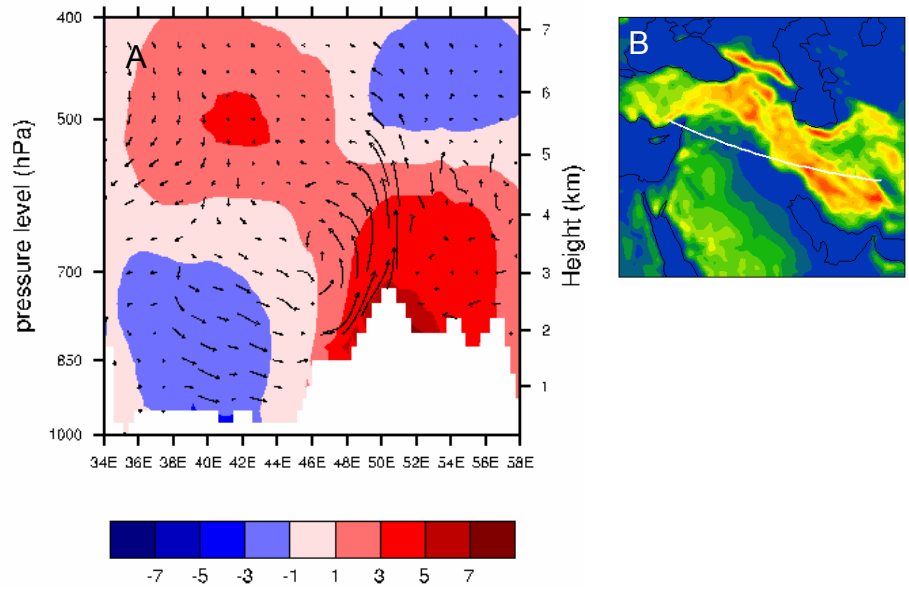

Figure 2: (A) Difference in the average July potential temperature (˚C), CONTROL minus MTSNOW, along a cross-section (B) drawn to capture major features of the anomalous circulation. The white feature along the bottom of (A) indicates topography. Vectors represent the difference wind field.

Model Derivation

Model I: Topography and boxcar heating with vertical shear

The goal is a three-dimensional, quasi-geostrophic circulation model that accounts for the combined influences of vertically-distributed heating and topography at the lower boundary. Atmospheric stability and the Coriolis parameters are treated as constants. Background wind is uniform in x and y, but vertical wind-shear is allowed.

We begin with Gill's (1982) form of the conservation of potential vorticity, along with the heat-forced tendency in potential temperature and the hydrostatic equation:

$$\rho_0 f_0^2 w_z = \frac{D_g}{Dt}\left(\nabla_H^2 P\right) \quad [1]$$

$$\frac{D_g \theta'}{Dt} + \left(\frac{N^2}{\alpha g}\right) w = \frac{q}{c_p \rho_0} \quad [2]$$

$$p'_z = g\alpha\rho_0\theta' \quad [3]$$

Following Bannon (1986), the vertical structure of *q* is defined as a step function, i.e.:

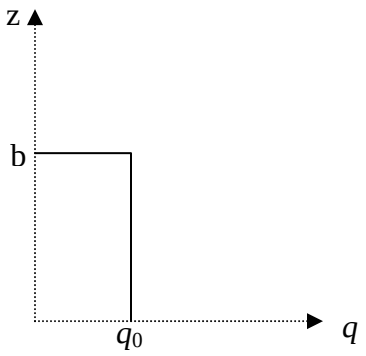

The lower boundary condition can thus be defined using [4] and the fact that at z=0, $w = \vec{U}_0 \cdot \nabla h$, where h=f(x,y) is the topographic forcing function:

$$\frac{1}{\alpha g \rho_0}\frac{D_g}{Dt} p'_z = \frac{q_0}{c_p \rho_0} - \frac{N^2}{\alpha g}\vec{U}_0 \cdot \nabla h \quad [4]$$

We can also define two boundary conditions at the interface height z=b:

$$\vec{U}_b \cdot \nabla_H \left(\Delta p'_z\right)\Big|_{z=b} = \frac{-\alpha g}{c_p} q_0 \quad [5]$$

and

$$\Delta p'\big|_{z=b} = 0 \quad [6]$$

For steady heating, the horizontal Fourier transforms of [4], [5], and [6] are, respectively:

$$i(\vec{k}\vec{U}_0 - i\delta)\hat{p}'_z - i(\vec{k}\vec{U}_S - i\delta)\hat{p}' = \alpha g \rho_0 \left(\frac{\hat{q}_0}{c_p \rho_0} - \frac{N^2}{\alpha g}\vec{U}_0 ik\hat{h}\right) \quad [7]$$

$$i\left((\vec{k}\vec{U}_0 - i\delta) + b\cdot(\vec{k}\vec{U}_S - i\delta)\right)\cdot\left(\Delta\hat{p}'_z\right)\Big|_{z=b0} = \frac{-\alpha g}{c_p}\hat{q} \quad [8]$$

$$\Delta\hat{p}'\big|_{z=b} = 0 \quad [9]$$

where $\vec{k}$ is the horizontal wave-number, δ is a Rayleigh damping term, and both *h* and q_0 are functions of (*x*,*y*). Solutions for the pressure field and perturbation wind fields are carried out in Fourier space and then transformed using the reverse FFT. In its general form, this model derives from that of Smith (1984).

Parameters applied to Model I are listed in Table 3. The horizontal structure of both heating and topographic forcing functions is a Gaussian ellipse, with maximum height, strength of heating, and the positioning of the forcing chosen to match the features of the Zagros Plateau (Figure 3a).

Model II: Vertically structured heating in the absence of shear

In order to obtain a closed form simulation for the case of heating in the presence of shear it was necessary to use a heating function that did not vary continuously with height. This is an unsatisfying simplification, so we also present the results of a quasi-geostrophic model in which vertical wind shear was neglected, but in which the scaled heating function is defined as:

$$B(x.y.z) = \frac{g}{\rho_0 c_p T_0} q_0(x,y)\cdot e^{-z/b} \quad [10]$$

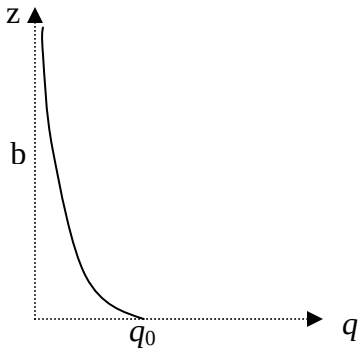

where $B(x,y,z)$ has units of m s^{-3}.

Governing equations are:

$$\vec{U} \cdot \nabla_H \vec{u}' - f\vec{u}' \times \vec{k} = -\nabla_H p' - \delta\vec{u}' \qquad [11]$$

$$0 = -p'_z + \beta \qquad [12]$$

$$\vec{U} \cdot \nabla_H \beta + N^2 w = B - \delta\beta \qquad [13]$$

$$\nabla_H \vec{u}' + w_z = 0 \qquad [14]$$

where β is buoyancy, $\vec{u}'$ is the perturbation in horizontal wind, and other terms are as defined previously. The equations are solved using Fourier transforms in *x*, *y*, and *z*, yielding:

$$\hat{p}'(k,l,m) = \left[\frac{(N \left|\vec{k}\right|)^2}{m\bar{\sigma}((N\left|\vec{k}\right|)^2 - m^2(\bar{\sigma}^2 - f^2))} - \frac{1}{m\bar{\sigma}} \right] \hat{B}(k,l,m) \qquad [15]$$

where *m* is the vertical wave number and $\bar{\sigma} = \vec{U} \cdot \vec{k} - i\delta$. Parameters used in this application are listed in Table 3.

Table 3: parameters used in the linear models

N	Brunt-Vaisala Frequency	0.01	s^{-1}
f	Coriolis Parameter	0.0001	s^{-1}
ρ_0	Air density at z=0	1.2	kg m^{-3}
U_0	Background wind (x)	10	m s^{-1}
T_0	Background surface Temperature	300	Kelvin
V_0	Background wind (y)	0	m s^{-1}
U_s	Vertical wind shear (x) -Model I only	0.002	s^{-1}
V_s	Vertical wind shear (y)	0.000	s^{-1}
b	Depth of heating	3000	m
h_{max}	Maximum mountain height -Model I only	0	m
q_{max}	Maximum heating rate	0.1	W m^{-3}
δ	Rayleigh damping term	0.00001	s^{-1}
dx,dy	Grid cell spacing	27	km
ax0	Source half-width (x)	6	cells
ay0	Source half-width (y)	12	cells
rot	Source rotation factor	-30	degrees

Significant Results

At altitudes above the height of direct heating, MM5, Model I, and Model II all predict the presence of high pressure and a persistent anti-cyclone (Figure 3). The magnitude of the high pressure anomaly is larger in the MM5 simulation than it is in either linear model, with a maximum of over 50 meters (or approximately 250 Pa), but this difference may be due to imperfect parameterization. Within the zone of heating (i.e., z < b), both MM5 and Model II predict an intense low pressure zone near the surface. Model I fails to produce a realistic surface low (see cross sections, Figure 4). This failure results from the use of a step function heating, for which q_z is zero at all heights other than *z*=*b*.

Cross sections do, however, indicate some advantage to including vertical wind shear. Where Model II locates the elevated high pressure system directly above the surface low, Model II (parameterized with positive wind shear) returns a downstream-tilting vertical pressure gradient that more closely resembles MM5 output (Figure 4a, compare with 4b and 2a). Obviously, in an environment where speed of the background wind increases with height, the realism of a model with a uniform wind field is severely limited.

Neither linear model reproduces the upstream cyclone observed in MM5 results (e.g. Figure 3d). Parameters can be adjusted to produce a small upstream anti-cyclone (not shown), but this feature is always substantially weaker than the paired anti-cyclone, and it is always displaced southward relative to the low pressure zone predicted by MM5. To date, then, linear models have provided some information on the mechanism of Zagros-induced circulations in the Middle East, but our understanding is far from complete.

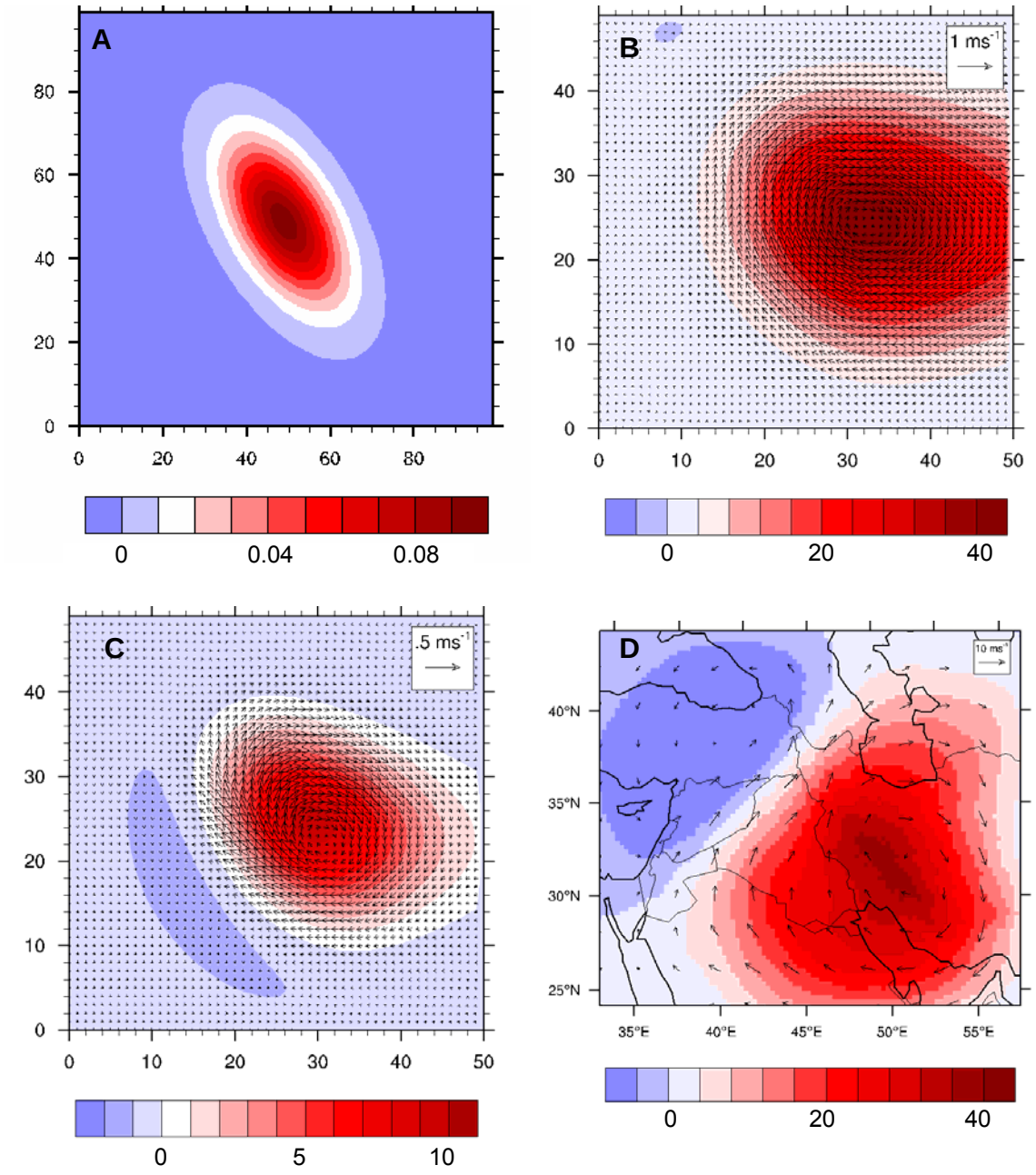

Figure 4: (A) Gaussian heating function at z=0. Units are W m^{-3}. (B) Pressure and wind perturbation at z=5000m for Model I, (C) the same fields for Model II. (D) Difference in the average August 500mb (approximately z=5000m) geopotential and wind fields, MM5 CONTROL minus MTSNOW. Units are Pa in (B) and (C) and meters in (D).

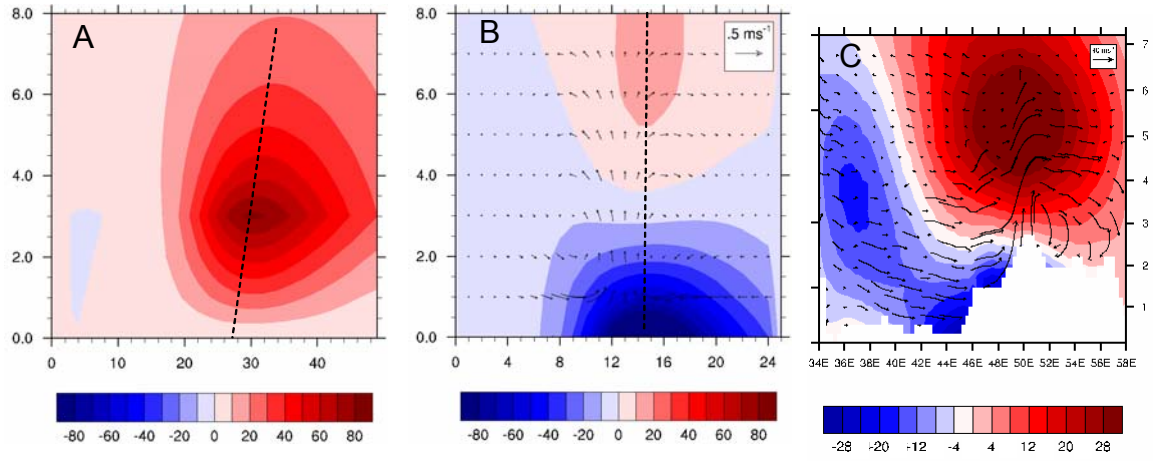

Figure 5: (A) Cross section of the pressure perturbation field at y=50 for Model I. Units are Pa. (B) The same cross section for Model II, with arrows indicating perturbation wind. (C) Average August geopotential height, MM5 CONTROL minus MTSNOW. Cross section is the same as in Figure 2 and units are meters. Units on the y-axis are km altitude in all panels. Dotted lines in (A) and (B) indicate the vertical orientation of the pressure perturbation.

References

Bannon, P.R., 1986: Linear development of quasi-geostrophic baroclinic disturbances with condensational heating. *J. Atmos. Sci.*, **43**, 2261-2274

Gill, A.E., 1982: Atmosphere-ocean dynamics. Academic Press, New York, 663 pages.

Rodwell, M.J. and B.J. Hoskins, 1996: Monsoons and the dynamics of deserts. *Q. J. R. Meteorol. Soc.*, **122**, 1385-1404.

Smith, R.B., 1984: A theory of lee cyclogenesis. *J. Atmos. Sci.*, **41**, 1159-1168.